# An Extended Closed Form of the ISRS GN Model for the Zero-Dispersion Regime

Filippos Balasis<sup>(1)\*</sup>, Daniel J. Elson<sup>(1)</sup>, Mindaugas Jarmolovičius<sup>(2)</sup>, Henrique Buglia<sup>(2)</sup>, Eric Sillekens<sup>(2)</sup>, Robert I. Killey<sup>(2)</sup>, Polina Bayvel<sup>(2)</sup>, Noboru Yoshikane<sup>(1)</sup>, Takehiro Tsuritani<sup>(1)</sup>, Yuta Wakayama<sup>(1)</sup>

- (1) KDDI Research, Inc., 2-1-15 Ohara, Fujimino 356-8502, Japan, xfi-balasis@kddi.com
- (2) Optical Networks Group, UCL (University College London), UK

**Abstract** The closed form approximation of the ISRS GN model is extended to include the multi-channel interference and accurately operate in the zero-dispersion regime. The derived equations are validated via comparisons with the split-step Fourier method and the integral form of the model. ©2024 The Author(s)

#### Introduction

In recent years, wideband transmission has emerged as a serious candidate system to facilitate the ever-growing need for more bandwidth. In addition to the expansion to bands located next to the C-band, coherent transmission in the Oband has shown promising potential since it can be achieved over a bandwidth that rivals that of S-C-L transmission with the use of a single type of bismuth doped fiber amplifier (BDFA) [1-4]. The zero-dispersion regime of O-band also lowers the complexity of the digital signal processing modules in the transceiver due to the absence of the dispersion compensation feature. However, this comes at the cost of significantly higher nonlinear interference (NLI) and, hence, requires the estimation of non-linear distortion.

The Gaussian noise (GN) model and the extended works that followed it [5-8] have been proven to be reliable tools albeit the focus so far has ranged from C-band-only to S-C-L WDM systems. In these works, the four-wave mixing (FWM), or multi-channel interference (MCI) as it is called in the GN model papers, has been mostly neglected due to the high dispersion present in these bands. A recent work, however, has demonstrated two significant points [9]. Firstly, the GN model remains valid in O-band when compared to split-step Fourier method (SSFM), and secondly, it is possible to calculate the integral form of the intra-band stimulated Raman scattering (ISRS) GN model within seconds by exploiting parallel computation in a cluster of powerful GPUs. Nevertheless, a closed form approximation of the model that considers MCI and the ISRS is still needed since it could be useful for fast NLI assessment and throughput optimization that could run on a moderate and accessible hardware.

This paper extends [8] by introducing a new  $\eta_{\text{MCI}}$  coefficient that estimates the MCI part in the presence of ISRS. The updated model is then compared to the integral form of the ISRS GN model, as well as to a SSFM simulation.

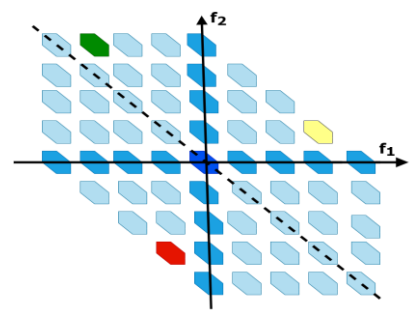


**Fig. 1:** The zero-dispersion frequency in this scenario is within the channel under test (dark blue island). The NLI contribution of each integration island is mostly determined by its closest high FWM efficiency axis. For example, green, red, and yellow islands are mostly affected by the  $f_1+f_2=0,\,f_1=0,\,$  and  $f_2=0$  axes, respectively.

## Phase mismatch in O-band

The GN model describes the accumulation of the NLI over the link via its link function and one of the critical terms in that function is the phase mismatch of the interfering frequencies. The closer to zero the mismatch, the more efficient the FWM becomes, leading to a higher level of NLI. The Taylor expansion of the propagation constant  $\beta$  at the zero-dispersion frequency provides some insight to that term in the O-band. In particular, the phase mismatch term  $\Delta\beta$  centered at the CUT becomes [5,8,10]

$$\Delta\beta=-4\pi^3\beta_3(f_1+f_2-2f_0)f_1f_2.$$
 (1) Equation (1) shows that phase mismatch becomes zero not only in terms of  $f_1$  and  $f_2$ , but also for

$$f_1+f_2-2f_0=0$$
, (2) where  $f_0$  is the location of the CUT with respect to the zero-dispersion. Figure 1 shows how the zero-dispersion causes the emergence of a third high FWM efficiency axis on the frequency plane, given by Eq. 2 and represented in this figure by the dashed line. To estimate the total MCI that affects the center frequency of the CUT, the link function must be integrated on all the rhombus-like islands that are not intersected by axes  $f_1=0$  and  $f_2=0$ . Equation (1) can be rewritten as

$$\Delta \beta = -4\pi^{3} \beta_{3} (\Delta f_{1} + \Delta f_{2} - 2f_{0} + f_{3}') \times (\Delta f_{1} + f_{1}') (\Delta f_{2} + f_{2}'), \tag{3}$$

where  $\Delta f_1$  and  $\Delta f_2$  are the frequency separations between the CUT and the corresponding interfering channels,  $|f_3'|=|f_1'+f_2'|\leq B/2$  and  $|f_1'|,|f_2'|\leq B/2$  with B being the symbol rate of the channels. One of the key steps in obtaining the extended closed form model (CFM) is restricting the double integration within an island to a single variable among  $f_1',f_2'$  and  $f_3'$ , chosen based on its proximity to the nearest high FWM efficiency axis, as shown in Fig. 1. The closest axis is found by

$$\min\{|\Delta f_1 + \Delta f_2 - 2f_0|, |\Delta f_1|, |\Delta f_2|\}.$$

Furthermore, as in [5,11], the integration of the link function is taken over squares that have equal area and the same geometric center as the rhombus shaped islands. This approach is also applied to the equations of XPM from [8] since  $\beta_3$  is extremely low and taking larger integrating area can lead to significant error. This leads to a redefinition of the integration domain limits to  $|f_1'|, |f_2'|, |f_3'| \leq \sqrt{3}B/4$ .

# Approximating the power profile of the MCI components

The second key point for the derivation of the CFM is the accurate estimation of the MCI components' power profile. In the presence of ISRS with uneven attenuation or a transmission bandwidth that exceeds the effective window of 15 THz, which in O-band are both true, a numerical method is required to provide fitted parameters that matches each channel's power profile. These parameters are then used as input in existing CFMs [8,12]. However, in the case of MCI, where three or four different channels are involved, it is computationally expensive to apply the same approach for each MCI component, considering that the total number of MCI terms is much larger than  $n^2$ , where n is the number of channels in the WDM signal. Instead, we present another method that provides an excellent approximation to the actual profile.

Along the lines of [8,12], the normalized power profile of a frequency f can be approximated as

$$\rho(z, f) = e^{g(z, f)},\tag{4}$$

$$g(z,f) = -a(f) \cdot z + \mathcal{C}(f) \frac{1 - e^{-\overline{a}(f)z}}{\overline{a}(f)},\tag{5}$$

where a(f), C(f) and  $\bar{a}(f)$  are the fitted parameters for that frequency f. Furthermore, by applying the ISRS GN model it can be shown that

$$\rho'(z, f, f_1, f_2, f_3) = \sqrt{\frac{\rho(z, f_1)\rho(z, f_2)\rho(z, f_3)}{\rho(z, f)}},$$
(6)

where  $\rho'(z, f, f_1, f_2, f_3)$  is the power profile of the MCI component for the corresponding frequencies  $f, f_1, f_2, f_3$ . Assuming the power profile of each MCI can also be expressed as in Eqs. (4)

and (5), we can define the corresponding parameters of an MCI term as  $\hat{a}$ ,  $\tilde{a}$ , and C'. Furthermore, assuming that the fitted parameters of each interfering channel in Eq. (6) are known in advance through a numerical method, the MCI parameters can be obtained by applying Eq. (6), for three different points in a fiber span of length L, specifically z=0, z=L/2, and z=L, and subsequently solving the system of equations.

#### The total NLI coefficient

Following the afore-mentioned steps and the assumption that the power profile of a channel re-

Table 1: Simulation parameters

Nonlinear coefficient γ [1/W/km]	2
Dispersion slope [ps/nm²/km]	0.087
Attenuation at 1305 nm [dB/km]	0.33
Attenuation slope [dB/km/nm]	-0.001
Symbol rate [GBd]	96
Channel spacing [GHz]	100
Number of channels	101
Zero-dispersion wavelength [nm]	1302.3
Center wavelength of WDM [nm]	1302.3
Length of span [km]	80

mains constant across its bandwidth, it can be shown that in a WDM signal with fixed channel spacing and symbol rate, the  $\eta_{\rm MCI}$  coefficient for an MCI that occurs in a channel with center frequency f is as follows

$$\eta_{\text{MCI}}(f, f_1, f_2, f_3) = \frac{16}{27} \frac{\sqrt{3}\gamma^2 K}{8\pi^3 \beta_3 S_2 S_3 \tilde{\alpha}(2\hat{\alpha} + \tilde{\alpha})B}, \tag{7}$$
 where  $f_1, f_2, f_3$  are center frequencies of the inter-

where  $f_1, f_2, f_3$  are center frequencies of the interfering channels such that  $f = f_1 + f_2 - f_3$ ,  $f \neq f_1$  and  $f \neq f_2 . S_1, S_2, S_3$  are elements of the sorted set  $\{|\Delta f_1 + \Delta f_2 - 2f_0|, |\Delta f_1|, |\Delta f_2|\}$  such that

$$S_1 \le S_2 \le S_3,\tag{8}$$

$$K = (R/\hat{a} - \hat{a}) \{ \arctan[\pi^3 \beta_3 S_2 S_3 (4S_1 + \sqrt{3}B)/\hat{a}]$$

$$-\arctan[\pi^3 \beta_3 S_2 S_3 (4S_1 - \sqrt{3}B)/\hat{a}] \}$$

$$+(A - R/A)\{atan[\pi^3\beta_3S_2S_3(4S_1 + \sqrt{3}B)/A]\}$$

$$-\text{atan}[\pi^3 \beta_3 S_2 S_3 (4S_1 - \sqrt{3}B)/A]\}, \tag{9}$$

$$A = (\hat{a} + \tilde{a}), \tag{10}$$

$$R = (\hat{a} + \tilde{a} - C')^2, \tag{11}$$

$$\hat{a} = (a_1 + a_2 + a_3 - a)/2 \tag{12}$$

$$\tilde{a} = -2\ln|D/T - 1|/L,\tag{13}$$

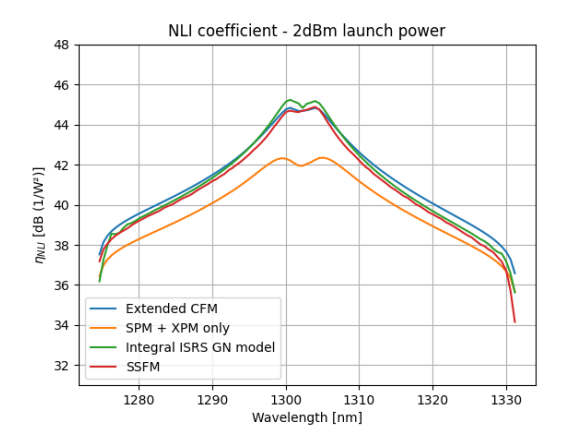
$$C' = D\tilde{\alpha}/(1 - e^{-\tilde{\alpha}L}), \tag{14}$$

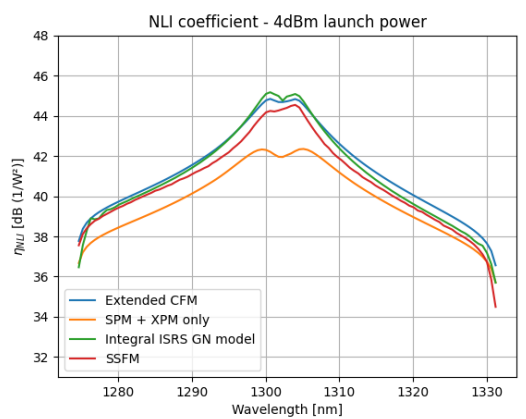
where a,  $a_1$ ,  $a_2$ , and  $a_3$  are the respective attenuation rates of the corresponding center frequencies. Here, we introduce parameters D and T as:

$$D = [C_1/\bar{a}_1(1 - e^{-\bar{a}_1 L}) + C_2/\bar{a}_2(1 - e^{-\bar{a}_2 L}) + C_3/\bar{a}_3(1 - e^{-\bar{a}_3 L}) - C/\bar{a}(1 - e^{-\bar{a}L})]/2,$$
(15
$$T = [C_1/\bar{a}_1(1 - e^{-\bar{a}_1 L/2}) + C_2/\bar{a}_2(1 - e^{-\bar{a}_2 L/2})$$

$$+C_3/a_3(1-e^{-\bar{a}_3L/2})-C/a(1-e^{-\bar{a}L/2})]/2,$$
 (16)

where  $\bar{a}$ ,  $\bar{a}_1$ ,  $\bar{a}_2$ , and  $\bar{a}_3$  are the respective fitted attenuation parameters of the involved channels in the Eq. (6).





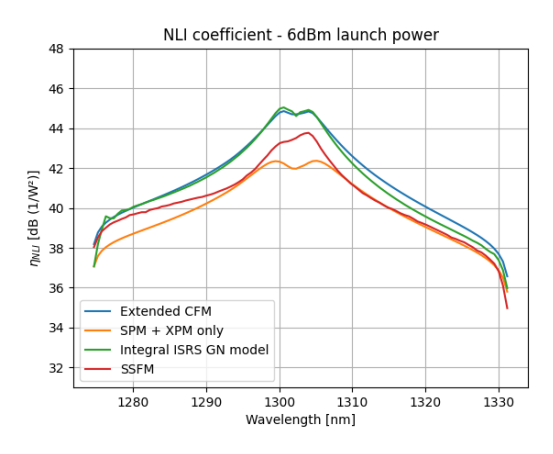


**Fig. 2** The NLI coefficients comparison includes data from the SSFM, the integral ISRS GN model, the CFM considering SPM and XPM only [8], and the extended CFM, for launch powers of 2, 4, and 6 dBm.

$$C$$
,  $C_1$ ,  $C_2$ ,  $C_3$  are respectively derived from  $C_i = P_T C r_i \Delta f_{ci}$ , (17)

where  $Cr_i$  is again the respective fitted parameter of the Raman gain slope [8],  $P_T$  the total power of the WDM signal and  $\Delta f_{ci}$  the respective distance from a reference frequency used for the estimation of the ISRS, usually located at the center of the WDM signal.

The coefficient for the total MCI on a center frequency f is

$$\eta_{\text{MCI}} = \sum_{i,j,k:f_i+f_j-f_k=f,f\neq f_i,f\neq f_j} \eta_{\text{MCI}}(f,f_i,f_j,f_k). \tag{18}$$
 Therefore, the coefficient of the total NLI is

$$\eta_{\rm NLI} = \eta_{\rm SPM} + \eta_{\rm XPM} + \eta_{\rm MCI},$$
where  $\eta_{\rm SPM}$  and  $\eta_{\rm XPM}$  are estimated as in [8].

## Accuracy of the proposed CFM

For the evaluation of the extended CFM's accuracy, we compared it with the integral form of the ISRS GN model, a SSFM and the CFM's version from [8] where MCI is not included. The parameters used in the simulation are given in Table 1. The comparison data of the SSFM and the integral ISRS GN model, where Gaussian constellation was assumed, were provided by UCL, using the same methods described in [9]. The fitted parameters were based on an actual Raman gain profile as in [9]. The plotted results are shown in Fig. 2. Results show a remarkable accuracy of the extended CFM compared to the integral ISRS GN model, especially in the shorter wavelength region. The mean absolute errors across the whole transmission bandwidth for three examined launched powers of 2, 4, and 6 dBm were 0.35, 0.34, and 0.32 dB, respectively. Compared to the SSFM, the mean absolute error was 0.48, 0.63 and 1.07 dB, respectively.

Furthermore, it is worth noting the absence of a tilt along the wavelength axis, something that is apparent in bands where dispersion is high. This can be attributed to the combined effect of ISRS and the zero-dispersion regime. In the case of S-C-L transmission the occurring NLI decreases when the spectrum distance from the respective interfering channels increases. However, in the zero-dispersion regime that's not the case anymore since NLI could still be large between distant channels as explained by Eq. (1). Both the integral ISRS GN model and the extended CFM managed to capture this phenomenon.

Finally, the discrepancy with the SSFM as the launch power increases can be explained by the GN model's derivation, which is based on the first order perturbation of the non-linear Schrödinger equation and the launch power as well as the non-linear coefficient are assumed to be low [9].

# Conclusions

We presented a novel extension of the closed form of the ISRS GN model accounting for and around the zero-dispersion regime to allow its application in the O-band. To the best of our knowledge this the first closed form approximation of the model where both the MCI and ISRS are considered. Comparison with the simulation results showed excellent overall agreement with the integral form of the model as well as with the SSFM for low to moderate launch powers. The next step would be to explore its accuracy in experiments.

# **Acknowledgements**

Support under UK EPSRC grants the EPSRC Programme Grant TRANSNET (EP/R035342/1), EWOC (EP/W015714/1) are gratefully acknowledged. MJ and HB acknowledge the support under a UCL, EPSRC (EP/T517793/1) and Microsoft Optics for the Cloud PhD scholarship.

#### References

- [1] Daniel J. Elson, Shohei Beppu, Ayumu Inoue, Daiki Soma, T. Nagashima, Vitaly. Mikhailov, Jiawei Luo, Sugizaki Takasaka, Dayrl Inniss, Noboru. Yoshikane, Takehiro Tsuritani, Tetsuya Hayashi, and Yuta. Wakayama, "115.2-THz aggregate bandwidth O-band coherent DWDM transmission over high-density 250-µm coating multicore fibre," 49th European Conference on Optical Communications (ECOC 2023), Hybrid Conference, Glasgow, UK, 2023, pp. 1662-1665, DOI: 10.1049/icp.2023.2661
- [2] Daniel J. Elson, Yuta Wakayama, Vitaly Mikhailov, Jiawei Luo, Noboru Yoshikane, Daryl Inniss, and Takehiro Tsuritani, "9.6-THz Single Fibre Amplifier O-Band Coherent DWDM Transmission," in Journal of Lightwave Technology, vol. 42, no. 4, pp. 1203-1208, 15 Feb.15, 2024, DOI: 10.1109/JLT.2024.3354083
- [3] Daniel J. Elson, Vitaly Mikhailov, Jiawei Luo, Shohei Beppu, Glenn Baxter, Ralf Stolte, Luke Stewart, Shigehiro Takasaka, Mindaugas Jarmolovi\v{c}ius, Eric Sillekens, Robert I. Killey, Polina Bayvel, Noboru Yoshikane, Takehiro Tsuritani, and Yuta Wakayama, "Continuous 16.4-THz bandwidth coherent DWDM transmission in O-band using a single fibre amplifier system," in Optical Fiber Communication Conference (OFC) 2024. Optica Publishing Group, Th4A.2, https://doi.org/10.1364/ofc.2023.Th4A.2
- [4] Vitaly Mikhailov, Member, IEEE, Yingzhi Sun, Jiawei Luo, Farooq Khan, Daryl Inniss, Yuriy Dulashko, Mark Lee, Joel Mann, Robert S. Windeler, Paul S. Westbrook, Jeffrey W. Nicholson, and David J. DiGiovanni, "1255-1355 nm (17.6 THz) Bandwidth O-band BDFA Pumped Using Uncooled Multimode 915 nm Laser Diode via YDF Conversion Stage." vol. 42, no. 4, pp. 1265-1271 2023, DOI: 10.1109/JLT.2023.3331325
- [5] Pierluigi Poggiolini, "The GN Model of Non-Linear Propagation in Uncompensated Coherent Optical Systems," in Journal of Lightwave Technology, vol. 30, no. 24, pp. 3857-3879, Dec.15, 2012, DOI: 10.1109/JLT.2012.2217729
- [6] Andrea Carena, Gabriella Bosco, Vittorio Curri, Yanchao Jiang, Pierluigi Poggiolini, and Fabrizio Forghieri, "EGN model of non-linear fiber propagation," Opt. Express 22, 16335-16362 (2014), DOI: <u>10.1364/OE.22.016335</u>
- [7] Daniel Semrau, Robert I. Killey and Polina Bayvel, "The Gaussian Noise Model in the Presence of Inter-Channel Stimulated Raman Scattering," in Journal of Lightwave Technology, vol. 36, no. 14, pp. 3046-3055, 15 July15, 2018, DOI: 10.1109/JLT.2018.2830973
- [8] Daniel Semrau, Robert I. Killey and Polina Bayvel, "A Closed-Form Approximation of the Gaussian Noise Model in the Presence of Inter-Channel Stimulated Raman Scattering," in Journal of Lightwave Technology, vol. 37, no. 9, pp. 1924-1936, 1 May1, 2019, DOI: 10.1109/JLT.2019.2895237
- [9] Mindaugas Jarmolovičius, Daniel Semrau, Henrique Buglia, Mykyta Shevchenko, Filipe M. Ferreira, Eric Sillekens, Polina Bayvel and Robert I. Killey. "Optimising O-to-U Band Transmission Using Fast ISRS Gaussian

- Noise Numerical Integral Model." arXiv preprint arXiv:2401.18022 (2024), DOI: 10.5522/04/24975612
- [10] K. Inoue, "Four-wave mixing in an optical fiber in the zero-dispersion wavelength region," in Journal of Lightwave Technology, vol. 10, no. 11, pp. 1553-1561, Nov. 1992, DOI: 10.1109/50.184893
- [11] Zefreh, Mahdi Ranjbar, and Pierluigi Poggiolini. "A closed-form approximate incoherent GN-model supporting MCI contributions." arXiv preprint arXiv:1911.03321 (2019) DOI: 10.48550/arXiv.1911.03321
- [12] Pierluigi Poggiolini and Mahdi Ranjbar-Zefreh, "Closed Form Expressions of the Nonlinear Interference for UWB Systems," 2022 European Conference on Optical Communication (ECOC), Basel, Switzerland, 2022, pp. 1-4, DOI: 10.48550/arXiv.2207.01001